HIGH-CURRENT LINEAR INDUCTION ACCELERATOR FOR ELECTRONS*

N. C. Christofilos, R. E. Hester, W. A. S. Lamb, D. D. Reagan, W. A. Sherwood, R. E. Wright
Lawrence Radiation Laboratory, University of California, USA
(Presented by N. C. CHRISTOFILOS)

INTRODUCTION

The key feature of the Astron concept [1] for containment and heating of the plasma is a cylindrical layer of relativistic electrons. A high intensity beam of electrons is injected in a cylindrical evacuated tank where an axially symmetric field is established by an external solenoidal coil. The injected electrons are trapped between two regions of enchanced field, oscillating back and forth along the evacuated tank. The electrons are injected in a field constant in time. In order to trap the injected electrons irreversibly it is necessary to absorb part of their energy as they move from the injection to the trapping region. This is accomplished by forcing a bunch of injected electrons to pass through a region filled with resistor rings located concentrically in respect to the electron bunch. Eddy currents generated in the resistors absorb part of the electron energy thus securing their trapping in the mirror field. In order to absorb a substantial portion of the electron energy it is required that the beam current be as high as 100 A. It is expected that an adequate number of electrons will be trapped so that the combined vacuum field and the electron layer field will form a pattern of closed magnetic lines wherein plasma can be trapped. Thereafter the plasma can be heated by Coulomb collisions with the relativistic electrons.

Therefore a high-current, high-energy electron accelerator is the key feature of a facility to test the Astron concept. After careful consideration the following parameters have been selected for the Astron accelerator which is now in operation.

Several tupes of accelerators were examined to determine their suitability for this application. First, it was decided that some form of linear accelerator was more appropriate than a machine using a circular guide field. Among the familiar types of linear accelerators is the travelling wave type [2], consisting of an iris-loaded waveguide operating at microwave frequencies. This was rejected as a solution on two counts: one was the power level required during the beam pulse; the other, perhaps fatally serious, was the detuning effect of such large currents in this type of accelerator [3]. Another familiar type of radiofrequency linear accelerator is the standing wave type, more usually used for ions [4]. Recently a machine such as this has been constructed for acceleration of high currents of electrons [5]. Because of our requirements for energy homogeneity and beam quality, preliminary designs did not seem attractive. The principle of magnetic induction when applied to a linear accelerator seemed to offer the most attractive solution to meet the requirements stated in Table 1.

Table 1

Parameters of Astron electron accelerator

Beam energy	4—5 MeV$\pm$0.5%
Beam current	200 A
Pulse length	0.25 μs
Repetition rate	0—60/sec
Beam quality	$<10^{-2}$ rad·cm

MAGNETIC INDUCTION PRINCIPLE

The principle of magnetic induction has been applied to the acceleration of electrons in the familiar betatron [6] and in the initial acceleration in the electron synchrotron [7]. In order to apply this to a linear accelerator, the geometry shown diagrammatically in Fig. 1 was utilized. A toroidal ring of magnetic material surrounds an accelerating column, and the change in flux in this magnetic core induces an axial electric field. The volt-seconds available to this system for a given magnetic material depends upon the cross-sectional area of the toroidal ring as indicated by the ex-

* Work performed under the auspices of the U. S. Atomic Energy Commission.

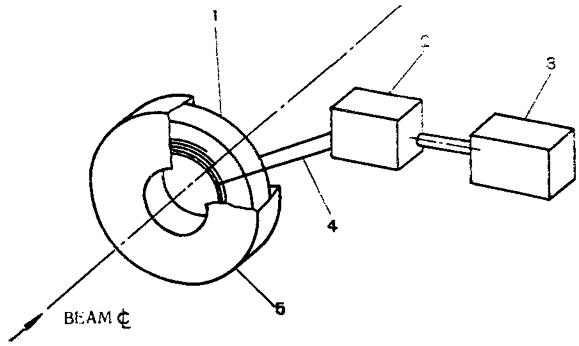

Fig. 1. Induction accelerator principle:
1 — laminated iron core; *2* — switch; *3* — pulse forming network; *4* — primary loop; *5* — secondary (case).

pression:

$$\oint \vec{E}\cdot\vec{dl} = -\frac{1}{c}\int_s \frac{\vec{dB}}{dt}\cdot\vec{ds}, \qquad (1)$$

where the particle to be accelerated performs the integration on the left side and the surface integral is taken over the cross section of the ferromagnetic material.

Hence, for a given weight of material, the beam pulse length influences the energy gain. Further, since it is the cross section that determines the energy available, a premium is put on minimizing the diameter for two reasons. The first is to minimize the total weight of magnetic material and hence its cost, and the

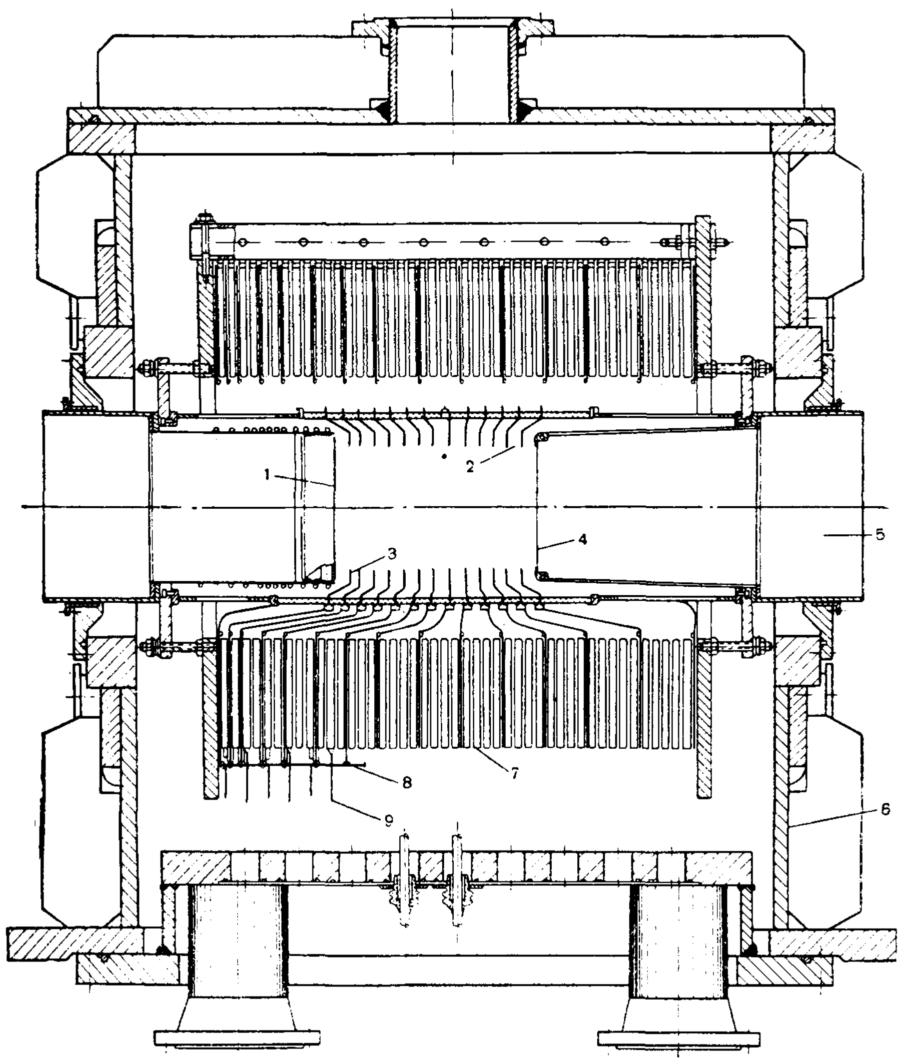

Fig. 2. Gun section. Astron 720 kV electron gun. *1* — 10″ cathode; *2* — brazed accelerator column; *3* — assembled accelerator column; *4* — grid; *5* — vacuum; *6* — pressure vessel 30 psig freon gas; *7* — iron cores; *8* — secondary; *9* — primary.

second is to minimize the power for magnetization which is also proportional to volume. The requirement for energy uniformity during the beam pulse makes it necessary to make some provision in the pulsing system to maintain a constant dB/dt during the useful part of the pulse. This can be done by providing a current ramp in the primary pulse. The choice of magnetic material was made by testing various samples to determine all of the properties which are important in **this** application. The material selected was 0.001-inch thick Ni — Fe tape wound into cores. The saturation flux of this material is 8,000 Gs, which permits a total flux change of 16,000 Gs.

THE ELECTRON GUN

The electron gun designed for this accelerator consists of a cathode and an accelerating system utilizing the induction principle. It is a requirement to minimize the transverse acceleration while the beam is at low energy. For this reason a 10-inch-diameter cathode

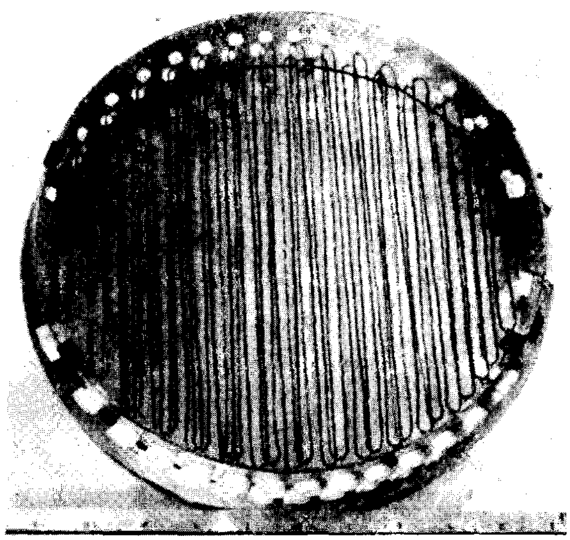

Fig. 3. Ten-inch cathode heater assembly.

was used; this results in an initial current density of the order of 1 A/cm^2. The required gradient is given by the Poisson equation for relativistic electrons in polar coordinates. A cross section of the gun assembly is shown in Fig. 2. The required field gradient is obtained by adjustment of electrode spacing and the number of cores between successive gaps. Each core contributes an average of 14 keV to the beam.

The entire gun assembly is installed in a pressure tank which is pressurized to two atmospheres of a mixture of Freon 12 and dry nitrogen. A blower circulates this gas through a heat exchanger to remove the heat generated in the system. The vacuum tube and the electrodes are constructed of 14-inch metal-ceramic seals in two parts which are welded together in the center.

The cathode is a conventional oxide cathode on a sintered carbonyl nickel base. It is heated by radiation on the heater assembly shown in Fig. 3.

Each core is threaded by three primary straps symmetrically placed and one monitor strap. Considerable attention was given during the development to insulating materials used in the assembly. Even though the spacings and voltages involved are conservatively chosen, the short pulses employed cause insulation failure and short lifetimes. Considerable testing was required before materials could be chosen whose service lifetime was judged satisfactory.

THE ACCELERATOR

The accelerator consists of the electron gun and 6 modular units of 48 cores each (Fig. 4). The accelerator modules are constructed around a metal-ceramic vacuum tube 6 in o. d. This tube is made up of eight electrode modules welded together into a continuous column. The core, primary straps and insulation are similar to those described previously for the gun; however, the cooling is by forced circulation of room air by means of blowers. The electric field across the accelerating gaps at radius r_0 can be expanded in a Fourier series,

$$E_Z = E_0 \sum_n a_n \cos(nkZ), \qquad (2)$$

where

$$k = 2\pi/s$$

and s is the distance between accelerating gaps. The free space wavelength corresponding to the pulse length is over a thousand times the diameter of the accelerating column Hence a solution of the Laplace equation is a good approximation of the field distribution. There-

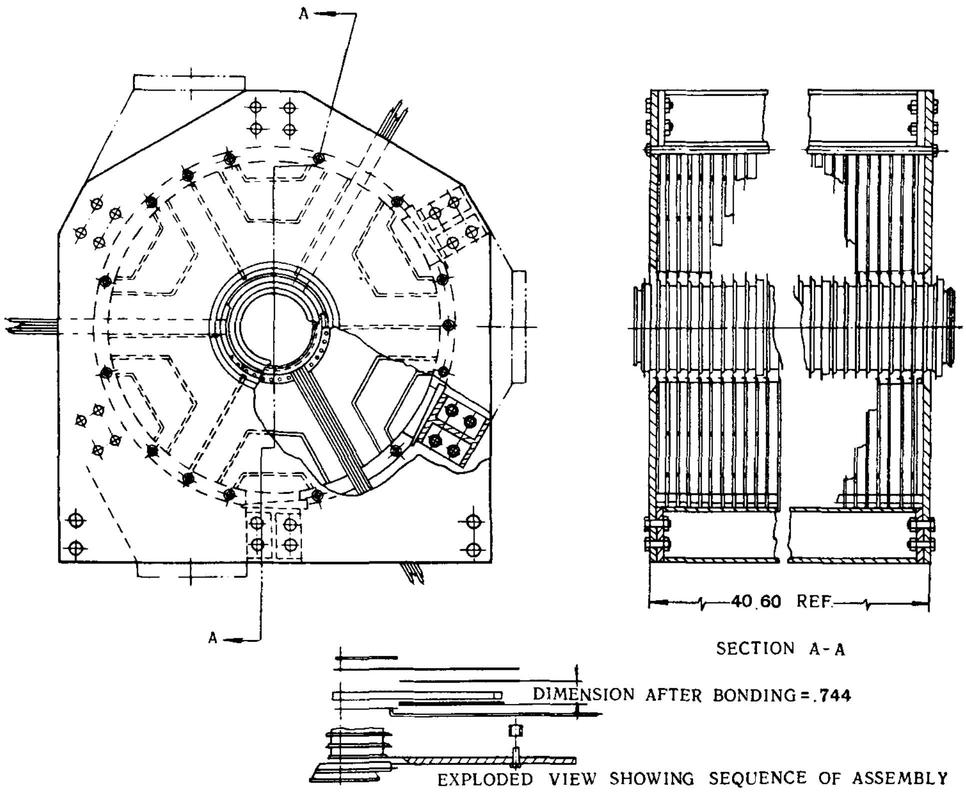

Fig. 4. Induction accelerator unit.

fore the electric field within the accelerating column is given by

$$E_Z = E_0 [1 + \sum_n a_n \beta_n I_0(nkr) \cos(nkZ)], \quad (3)$$

where

$$\beta_n = [I_0(nkr_0)]^{-1}.$$

All the higher harmonics of this solution are undesirable, and they must be suppressed to a small value. By selecting the radius r_0 of the electrode rings about twice the beam radius, and the accelerating gap about three to four times smaller than the radius r_0, the higher harmonics are suppressed to about 1% of the accelerating field. One of the requirements of the accelerator is that the final beam radius be about 1 cm, therefore additional focusing is required. As a high-current electron beam is accelerated to energies where relativistic effects are important the magnetic forces associated with the beam's self-magnetic field become very nearly equal to the electrostatic forces due to the charged particles in the beam. The net force in the absence of positive charge is always repulsive but it is diminished by the factor γ^{-2}, where γ is the ratio of the electron's relativistic mass to its rest mass. Therefore as the beam is accelerated it is periodically focused with solenoidal lenses until the final beam radius of about 1 cm is achieved.

THE PULSER SYSTEM

The electronic system for this type of accelerator is really what finally determines the performance and reliability of the machine. The basic requirements are to induce the maximum practical flux change in each core and as far as possible maintain a constant flux change and consequently a constant electric field during the useful part of the pulse. Fig. 5 is a block diagram of the components of the system adapted for use on this machine with the general specifications and waveforms when appropriate. The development of this equipment is discussed in a previous publication [8]; however, the following is a brief description of the function of the system.

Table 2 lists the chief performance requirements of the pulser system.

Table 2

Typical core pulsing requirements

Item	Gun core	Accelerator core
Peak primary voltage*, V	16,000	12,000
Peak input current*, A	4,500	1,800
Peak power input*, MW	70	21.6
Maximum input impedance, Ω	12.5	17.5
Minimum input impedance, Ω	2.9	6.0
Primary voltage rise time, ns	40	40
Secondary voltage rise time, ns	40	40
Primary voltage fall time, ns	60	60
Secondary voltage fall time, ns	60	60
Pulse duration over ±0.50% portion (μs)	0.25	0.25

* Measured at the end of the 0.25-μs flat region of pulse.

have to be long enough so that the reflection due to mismatch at the load would not arrive during the pulse; hence the minimum length was 130 feet. Several milliseconds before the pulse forming networks are charged, each core is taken into saturation in the negative direction by a reset pulse of 50 A which persists for 200 μs. This ensures that all the volt-seconds available in each core can be used efficiently when the thyratron switch chassis are fired. Fig. 5 shows a schematic of the pulse shaper chassis. These are devices in parallel with the cores that store energy early during the pulse and deliver the stored energy late in the pulse. This produces a current ramp which can be adjusted to give the required ± 0.5% voltage pulse from each core.

PRELIMINARY ACCELERATOR OPERATION

All the preliminary operation has been at 5 pps (pulses per second). The accelerator has produced average currents of 120 A for pulse durations of 0.3μs. The peak currents as shown

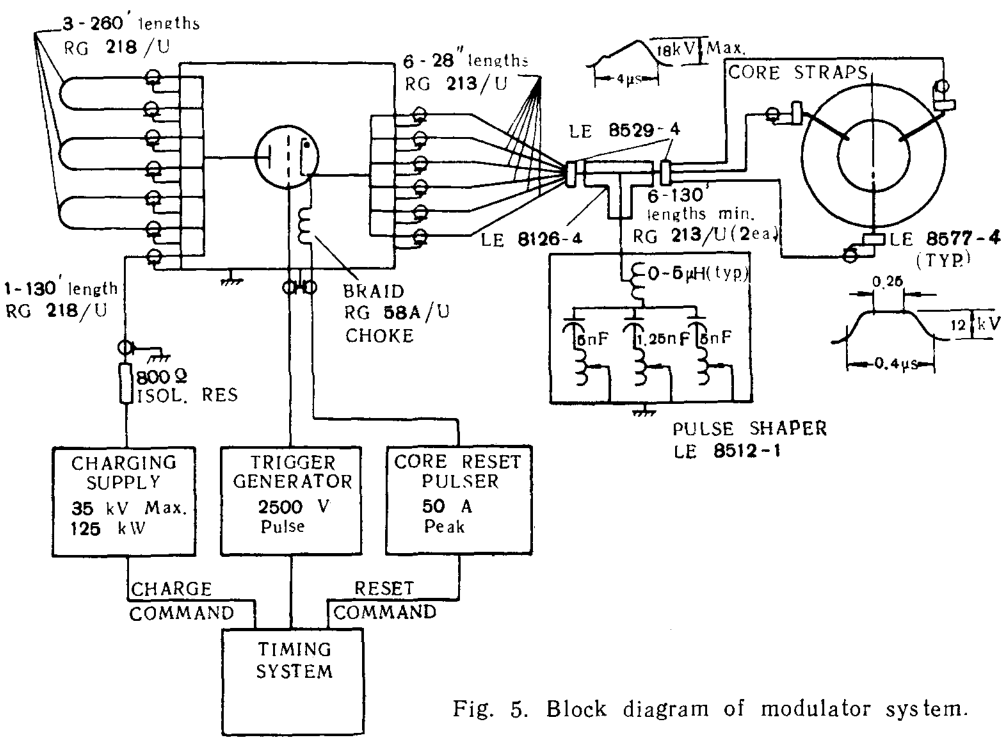

Fig. 5. Block diagram of modulator system.

Resonant charging of the energy storage cables was chosen to minimize the time of maximum voltage stress. The output cables in Fig. 6 are about 160 A; however, the current pulse amplitude is not constant in time, and the average is 120 A. The current pulses are monitored in a deep Faraday cup which has a 50 Gs transverse magnetic field at the back of the cup. This magnetic field is sufficient to trap all low-energy secondary electrons and the small solid angle is relied on to reduce the effect of escaping backscattered primary electrons. The current is monitored by measuring the voltage produced across a very low inductance 0.5 Ω resistor attached to the Faraday cup.

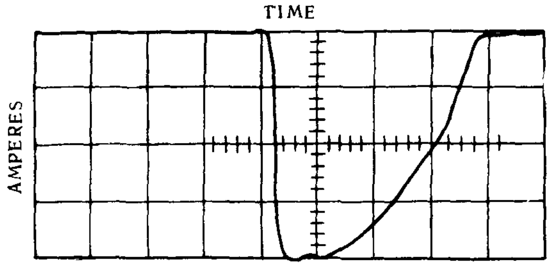

Fig. 6. Beam current pulse monitored by a Faraday cup (40 A/cm, 0.1 μs/cm).

The beam energy has been measured to be 4.0 ± 0.1 MeV. The energy was determined in two ways. One method is a calorimetric measurement using a water-cooled Faraday cup. Another method involves adding up all the voltage pulses from the core monitor straps. Each core has a precision voltage divider attached to its monitor strap. These voltage dividers were calibrated by turning off accelerator units and individual cores until the threshold for the photodisintegration of deuterium was established.

The initial operation of the full accelerator commenced in mid-February, 1963. The accelerator consists of the electron gun and six accelerator units. This requires the simultaneous of 333 cores and 423 switch chassis. Each gun core requires three switch chassis. Four hund-

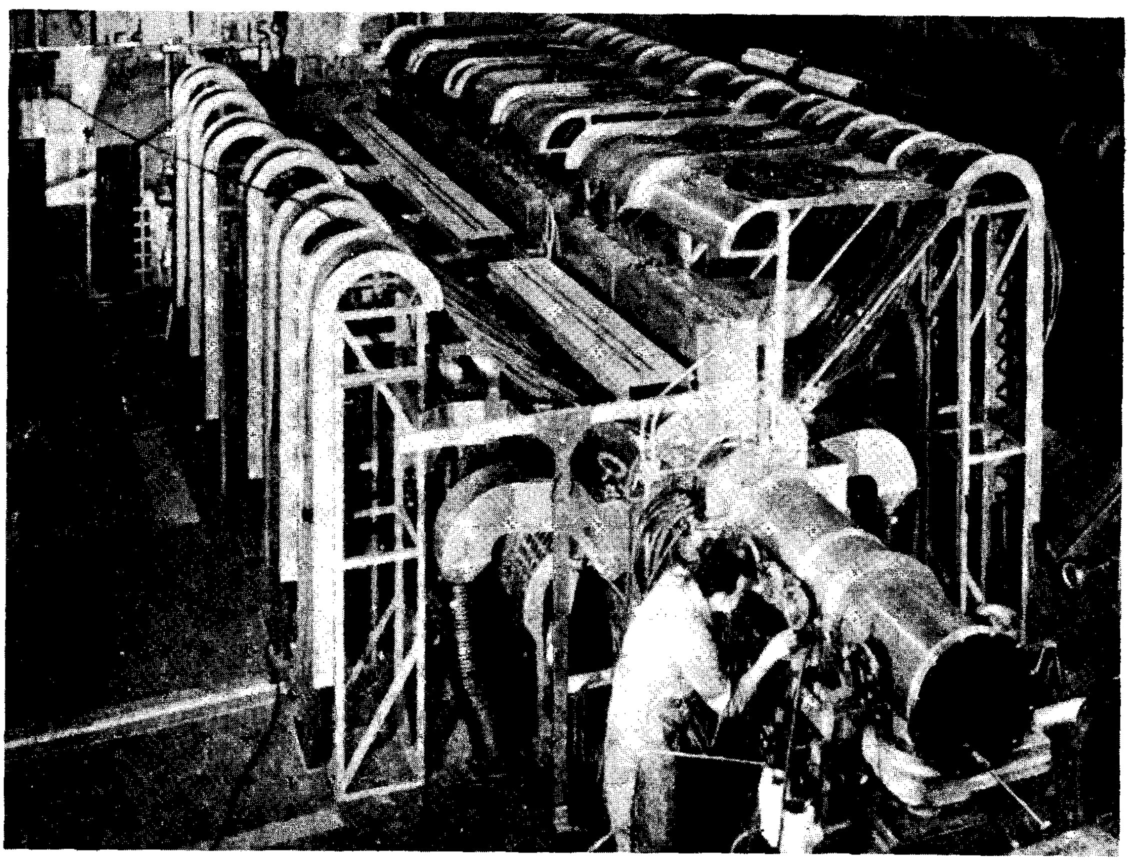

Fig. 7. Overhead view of the Astron accelerator as it appeared when first put into operation.

red hours of operating time at 5 pps has established a mean time to failure of about 4 h. It is expected that the mean time to failure can be improved. However, the accelerator consists of many modular units and the failure of a module only removes one core from operation. This results in less than 1% beam energy loss, therefore a failure during operation need not terminate an experiment. Fig. 7 shows an overhead view of the Astron accelerator as it appeared during initial operation.

REFERENCES

1. Christofilos N. C. Astron Thermonuclear Reactor. In: Proceedings of the Second UN International Conference on the Peaceful Uses of Atomic Energy, vol. 32 (Geneva, 1958), p. 279.
2. Christofilos N. Astron Electron Injection Lawrence Radiation Laboratory (Livermore) Rept. UCRL-5617-T, June 22, 1959.
3. Chodoroiv M., Ginzton E. L., Hansen W. W., Kykl R. L., Neal R. B. and Panofsky W. K. H. Rev. Scient. Instrum., **26**, 134 (1955).
4. Khizhnyak N. A., Tolok V. T., Chechkin V. V. and Nazarov N. I. J. Nucl. Energy, Part C, **4**, 129 (1962).
5. Smith L. In: Encyclopedia of Physics, Nuclear Instrumentation I (Springer-Verlag, Berlin, 1959), Vol. XLIV, p. 341.
6. Venable D. Rev. Scient. Instrum., **4**, 456 (1962).
7. Kerst D. W. Phys. Rev., **60**, 47 (1941).
8. Smith V. L. IRE Trans. Nucl. Sci., NS-9, 57 (1962).